New analysis of the temperature-dependent threshold density for electron self-trapping in gaseous helium

A. Borghesani, Nelly Bonifaci, A. Khrapak, V. Atrazhev

New analysis of the temperature dependence of the threshold density for electron self-trapping in gaseous helium

Armando Francesco Borghesani,*[a] Nelly Bonifaci,[b] Aleksei G. Khrapak,[c] and Vladimir M. Atrazhev[c]

We present the results of a new analysis of the literature electron mobility μ data aimed at determining the exisyence of a threshold density for electron self-trapping in gaseous helium as a function of temperature.We have investigated the density dependence of μ and, when available, its dependence on the electric field. The data deduced from the experiments are favorably rationalized by minimizing the excess free energy of the self-localized states within the *optimum fluctuation model*. It is shown that the formation of electron bubbles via the self-trapping phenomenon is determined by the delicate balance between the electron thermal energy, the density dependence of the electron energy at the bottom of the conduction band in the gas, and the isotherm work necessary to expand the bubble. We, thus, show that the self-trapping phenomenon is not restricted to low temperatures but can occur at any temperatures for a large enough density.

1 Introduction

The dynamics and energetics of electrons in disordered systems has long since been investigated because of their scientific relevance. Rare liquids and gases are the simplest possible realization of a disordered system, in which the study of electron transport can shed light on the behavior of electrons in such media.

Electrons injected into dielectric liquids or gases, in which the electron-atom interaction is dominated by short-range repulsive exchange forces, can locally deform the compliant fluid so as to give rise to a new state that cannot be adiabatically obtained as a result of a simple addition of an electron to the host medium. Under certain thermodynamic conditions, electrons may stabilize the locally deformed host structure and self-localize in empty, or even partially filled, cavities, which are simply termed electron bubbles, whose radius is of the order of 2 nm.

Under the action of an externally applied electric field, electron bubbles very slowly drift through the medium because of their very large hydrodynamic mass, their drift velocity being several orders of magnitude smaller than that of quasi-free electrons in gases or liquids of comparable density, in which the electron-atom interaction is not as repulsive.

Localized electron states have first been observed in liquid helium that is by far the most investigated system.[1] Electron bubble states have then been discovered in dense gaseous helium at low temperature,[2] and are also been proved to occur in liquid neon,[3,4] in dense neon gas[5,6], in methanol [7] and ammonia gas,[8,9] in nitrogen vapor,[10], in liquid hydrogen,[11–13], in water vapor,[14] and also in some liquid hydrocarbons.[15] A direct confirmation of the existence of electron bubbles in liquid helium has further been produced by means of very elegant spectroscopic experiments.[16,17]

A sufficiently simple model system to investigate has always been helium gas at low temperature. Historically, the formation of electron self-trapped states has been inferred by the analysis of the behavior of the electron drift mobility μ as a function of the medium density N. A sharp transition from high- to low mobility has always been considered the fingerprint indicating the presence of localized electron states.[2,18] However, high density measurements in helium at higher temperatures [19–21] and in neon close to the critical temperature[6] have shown that the mobility drop is all but an extremely sharp one. It rather shows a gradual transition from high values at low density to very low values at high density, thereby leading to the conclusions that: i) the observed mobility is a statistical average of the mobility of the highly mobile, quasi-free electron states and of that of the slow localized ones, ii) the electron self-trapping phenomenon is not limited to low temperatures, iii) localized and quasi-free states do coexist, though in different proportions, in almost all experimentally investigated conditions, iv) the relative fraction of the two populations is ruled by statistical mechanics and, hence, by

[a] *CNISM Unit, Department of Physics & Astronomy, Università degli Studi di Padova, 35131 Padua, Italy, E-mail: armandofrancesco.borghesani@unipd.it*
[b] *G2Elab, CNRS/Grenoble INP/Université Grenoble Alpes, 38000 Grenoble, France*
[c] *Joint Institute for High Temperatures, Russian Academy of Sciences, 125412 Moscow, Russia*

both the electron energy levels in the gas and by the gas thermodynamics.

A still debated question is whether self-localized states can only appear unless a critical density is reached or if they are always present at any density and temperature. Over the years, this question has received controversial anwers: some researchers pointed out that there is no need to consider the initial drop-off of the mobility as a function of the density and the localization as distinct phenomena, thereby implying that localized - and quasi-free states always coexist[2,18,20]. Others scholars make the hypothesis that localized states can only exist if some critical, temperature dependent density is exceeded.[4,19–24]

Actually, the quasi-free mobility, even at low density and high temperature, shows large deviations[25–29] from the prediction of the classical kinetic theory[30] because the electron thermal wavelength is larger than or comparable to the electron mean free path and to the average interatomic spacing, thereby leading to multiple scattering effects. Owing to this fact, from an experimentalist point of view a better way to answer the previous question is to investigate if there is a critical density, above which the measured mobility significantly deviates from the predicted behavior for quasi-free electrons.

To this goal and to correctly explain the graduality of the mobility drop as a function of the density at constant temperature an accurate description of the density dependence of the mobility of both the quasi-free electrons and the electron bubbles is required. In relatively recent years a heuristic model has been developed that correctly describes the density, temperature, and electric field dependences of the mobility of quasi-free electrons in noble gases[31–33]. Even more recently, this model has been applied to helium gas with great success.[34] The model incorporates into the classical kinetic picture the three most important multiple scattering effects: i) a density dependent energy shift of the electron kinetic energy $V_0(N)$, known as the minimum energy at the bottom of the conduction band in the gas[23,24], ii) a quantum self-interference effect that enhances the electron backscatttering rate[29,35] and leads to the presence of a mobility edge (known as *weak localization*)[36], and iii) a static structure factor related enhancement of the scattering cross section due to correlations[37].

With the aid of this new and accurate description of the mobility of quasi-free electrons it is now possible to reanalyze experimental data that can be found in literature that were spoiled by the absence of an accurate knowledge of the behavior of the quasi-free electrons. We will show that electron bubbles form at any temperatures whenever their free energy is favorable as can be detected by inspecting the deviations from the predicted quasi-free mobility.

Moreover, some new pieces of information can be gathered from experiments in which the electric field dependence of the electron drift velocity is measured because of the ability of the heuristic model to describe it.

In this paper we will address the question if a critical density is required for the onset of the localization phenomenon by comparing the results of the analysis of the experimental outcome with the numerical results obtained by minimizing the excess free energy ΔA we compute by adopting the *optimum fluctuation model*. We wil assume that electrons bubbles are described by potential wells with a square profile. This simplistic hypothesis is, however, sufficient for our goals as potential wells with rounded walls or with self-consistently detemrmined profiles computed by using density functional methods do not produce too different results.

The paper is organized as follows. In Section 2 we show the experimental evidence supporting the idea that there is a threshold density for the detection of electron bubbles from mobility measurements. In Section 3 we describe physics of the optimum fluctuation model and carry out the related computations leading to numerical results that are compared to the experimental outcome. Finally, some conclusions are drawn in Section 4.

2 Experimental phenomenology

The electron mobility μ in gaseous helium has thoroughly been investigated over the course of many years by using different techniques. Although some experiments were aimed at investigating the deviations of μ from the prediction of classical kinetic theory whereas some others were mostly interested to shed light on the properties of electron bubbles, nonetheless the experiments span over sufficiently broad temperature and density ranges to cover both limiting behaviors and also the transition region in which quasi-free- and self-trapped states coexist.

In some experiments[2,18,21,26], the dependence of the electron drift mobility $\mu(E)$ on the drift field E has been investigated, in addition to its dependence on density and temperature. From these experiments we can deduce the so-called *zero-field* mobility $\mu_0 = \lim_{E\to 0}\mu(E)$, i.e., the value of the mobility at thermal energy. In other experiments[19,38], only μ_0 has been measured as a function of density and temperature. In the former cases, we will show that pieces of information about the onset of the self-trapping phenomenon will be gathered from the behavior of μ as a function of E, whereas in the latter cases we will have to look at the deviations of μ_0 from the behavior predicted by the heuristic model.

2.1 Density effects

We show in Fig. (1) a collection of all literature measurements of the thermal mobility μ_0 as a function of N for temperatures in the range $4.2\,\mathrm{K} \le T \le 77.6\,\mathrm{K}$. For all T except the highest, the transition from high- to low mobility is almost complete. As we can see, even at the lowest temperatures the mobility drop is far from being very sharp. The transition is gradual and it makes difficult to detect a threshold density for self-trapping only from the density dependence of μ_0 at constant temperature.

More detailed pieces of information can be obtained from experiments, in which μ has been measured as a function of the drift electric field E. In Fig. (2) we show the behavior of the density-normalized mobility μN as a function of the reduced electric field E/N fot $T = 4.2\,\mathrm{K}$[18] and $T = 26.1\,\mathrm{K}$[34]. Similar behavior has been observed at low T[2] as well as at higher T[21,26], and also in neon gas close to its critical temperature.[6] By increasing N, the field dependence of μ changes. At low N and E, μ is constant as a function of E and takes on its corresponding thermal value μ_0, or $\mu_0 N$ for the density-normalized mobility. In this region, the heuris-

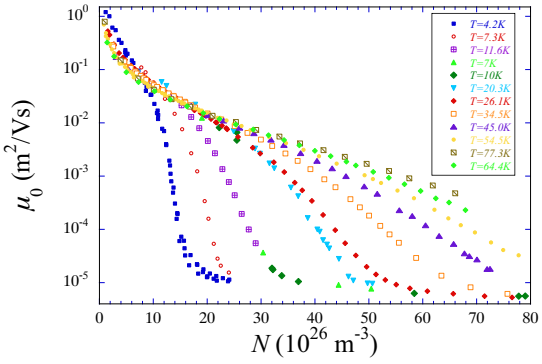

Fig. 1 Collection of the zero-field mobility measurements μ_0 as a function of the density for several temperatures. Closed blue squares: $T = 4.2\,\mathrm{K}$ [2,18,19]. Open red circles: $T = 7.3\,\mathrm{K}$ [19]. Lilla crossed squares: $T = 11.3\,\mathrm{K}$ [19]. Light green triangles: $T = 7\,\mathrm{K}$ [38]. Dark green closed diamonds: $T = 10\,\mathrm{K}$ [38]. Turquoise inverted triangles: $T = 20.3\,\mathrm{K}$ [20]. Red closed diamonds: $T = 26.1\,\mathrm{K}$ [21]. Orange open squares: $T = 34.5\,\mathrm{K}$ [21]. Lilla open triangles: $T = 45.0\,\mathrm{K}$ [21]. Lilla triangles: $T = 45.0\,\mathrm{K}$ [21].Yellow closed circles: $T = 54.5\,\mathrm{K}$ [21]. Light green diamonds: $T = 64.4\,\mathrm{K}$ [21]. Brown barred squares: $T = 77.3\,\mathrm{K}$ [26].

tic model for the mobility accurately describes the density and temperature dependence of $\mu_0 N$ by taking into account multiple scattering effects.[31,34] At higher field, electrons become epithermal, the electron wavelength becomes shorter, and the influence of multiple scattering effects is reduced. As a consequence, the experimental μ data smoothly and monotonically converge to the $(E/N)^{-1/2}$ behavior predicted by the classical kinetic theory.[30]

However, if a temperature dependent value of the density, $N_{\mathrm{th}}(T)$, is trespassed, the mobility at first increases over its thermal value as the field is increased and goes through a maximum before converging to classical $(E/N)^{-1/2}$ behavior. As for $N < N_{\mathrm{th}}$ the heuristic model, obtained from the classical kinetic theory expression dressed by the effects of multiple scattering, accurately describes both the density and electric field dependence of μ,[34] we claim that the change mobility behavior is associated with the appearance of self-trapped state in nonnegligible proportion. We will assume that the threshold density N_{th} is located by this change behavior of the mobility.

In Fig. (3) we plot the values of the threshold density N_{th} obtained from several experiments. In the case of the experiments in which only the zero-field value μ_0 was measured[19,20,38], the threshold density has been determined by computing the ratio of the measured μ_0 to the value predicted by the heuristic model. The lines in this figure represent the curves corresponding to a given fraction of self-trapped states, as described in the caption, and are computed by adopting the optimum fluctuation model, whose details will be described in the next sections. For instance, the dash-dotted line is the locus of points for which the fraction of self-trapped states amount to 2%. As soon as the density is higher than the threshold density at a given temperature, the fraction of localized states becomes non negligible and produces a measurable effect on the observed mobility according to eqn (12) and eqn (13). From this curve it is evident that self-trapped states can be present at any temperatures, provided that the density is large enough.

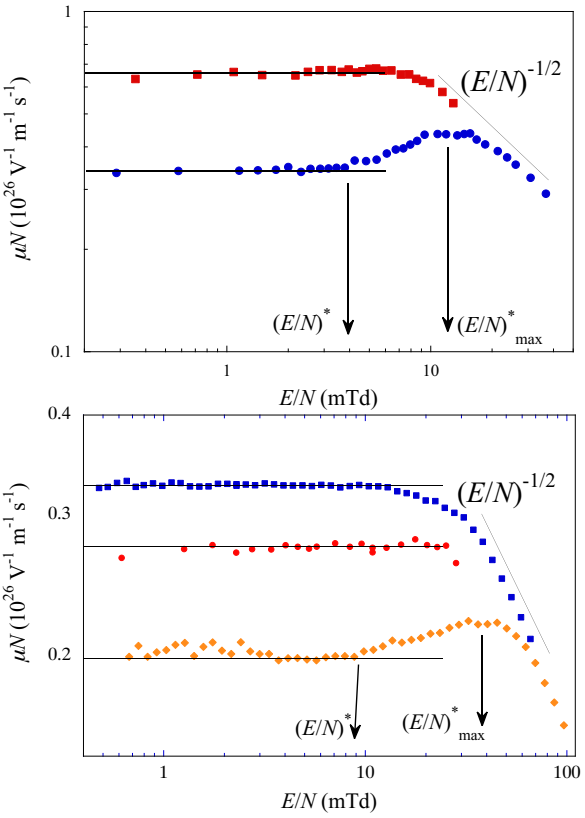

Fig. 2 Reduced electric field E/N dependence of the density normalized mobility μN for some N and T. Top panel: $T = 4.2\,\mathrm{K}$ for $N = 7.5$, and 9.5 (from top).[18] Bottom panel: $T = 26.1\,\mathrm{K}$ for $N = 17.3$, 19.5, and 22.8 (from top).[21,34] N is expressed in units of $10^{26}\,\mathrm{m}^{-3}$ and E/N in mTd ($1\,\mathrm{mTd} = 10^{-24}\,\mathrm{Vm}^2$). At low E/N, μN is independent of E/N. At high field, the classical kinetic theory predicts a $(E/N)^{-1/2}$ behavior. The arrows indicate the value $(E/N)^\star$, at which μN starts increasing over its thermal value, and the field value at the mobility maximum $(E/N)^\star_{\mathrm{max}}$.

The experimental results[19] shown as crosses in Fig. (3) deserve a comment. In this case, μ was not measured as a function of E but only the thermal value μ_0 was measured. The density dependence of μ_0 at low- to intermediate density values, where no localization still takes place, does neither obey the heuristic model predictions nor agrees with more accurate experimental data[18]. Moreover, those data were normalized to the prediction of the classical kinetic theory, which is much higher than the correct prediction of the heuristic model. For these reasons, the only experimental results that can reliably be considered are those, in which the mobility is so low as to be attributed with certainty to electron bubbles.

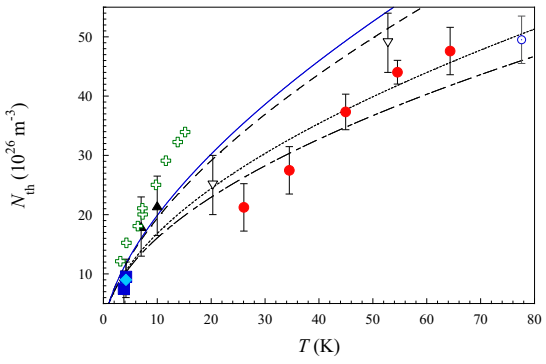

Fig. 3 Temperature dependence of the threshold density N_{th} for electron self-trapping from several experiments. Squares[18], closed circles[21], triangles[38], inverted triangles[20], diamond,[2], and open circle.[26] The lines are the locus of points of constant localized states fraction ϕ. Dash-dotted line: $\phi = 2\%$, dotted line: $\phi = 5\%$, dashed line: $\phi = 50\%$, solid line: $\phi = 60\%$. Along the $\phi = 50\%$ line localized states and quasi-free states are equiprobable. The crosses[19] correspond to a situation in which almost only electron bubbles contribute to the overall mobility and can be assumed to represent the $\phi \approx 100\%$ case.

2.2 Electric field influence

A picture coherent with the data presented in Fig. (2) and in Fig. (3) is obtained by analyzing the behavior of the threshold electric fields $(E/N)^\star$, or equivalenty $E^\star$, and $(E/N)^\star_{\max}$, or $E^*_{\max}$, as shown in Fig. (2). In Fig. (4) we report the values of the threshold field $E^\star$ as a function of N for some low-, intermediate-, and high temperatures. $E^\star$ increases linearly with N. (For even higher N, $E^\star$ increases superlinearly with N.) The extrapolation to $E^\star = 0$ leads to a determination of the threshold density N_{th} consistent with the values reported in Fig. (3).

A further indication of internal coherence can be obtained by inspecting the density dependence of $E^\star$ and $E^\star_{\max}$, shown in Fig. (5). Similar behavior is observed at all temperatures. Within the experimental accuracy, both quantities extrapolate to zero for the same threshold density, thereby supporting the claim that both the initial deviation form the thermal value μ_0 and the initial occurrence of a mobility maximum are related to the onset of formation (or, at least, of detectability) of localized states.

Let us consider the effect of the electric field on the electron energy distribution. It is well known that the electric field acts so as to enhance the average electron energy over its thermal value. It has been shown that more energetic electrons are less prone to get self-trapped.[40] A shift of the electron energy distribution function to higher energies due to the action of the field leads to an increase of the quasi-free electron fraction with respect of the localized ones.

It is therefore important to ascertain how multiple scattering effects do compete with the electric field to thermalize electrons so that they can more easily get localized. To this goal, it is instructive to see how the classical kinetic theory and the heuristic model perform at describing the electric field dependence of the

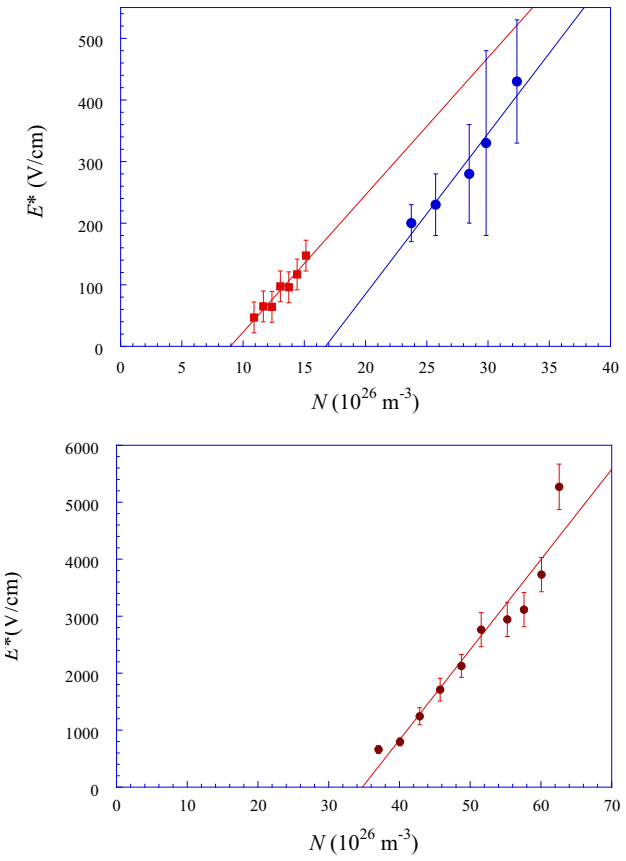

Fig. 4 Density dependence of the threshold electric field $E^\star$. Top panel: $T = 4.2\,\mathrm{K}$[18] (red squares) and $T = 26.1\,\mathrm{K}$[21] (blue circles). Bottom panel: $T = 45.0\,\mathrm{K}$[39]. The lines are linear fits to the data.

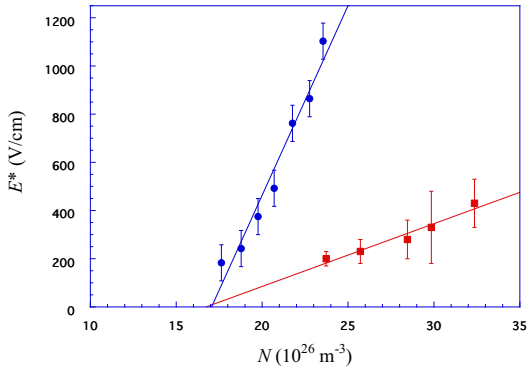

Fig. 5 Density dependence of $E^\star$ (red symbols) and $E^\star_{\max}$ (blue symbols) for $T = 26.1\,\mathrm{K}$. The lines are linear fits to the data.

measured mobility for a density close to N_{th}.

To this goal, we compare in Fig. (6) the prediction of the heuristic model with data at $T = 4.2\,\mathrm{K}$ and $N = 9.48 \times 10^{26}\,\mathrm{m}^{-3}$.[18] The

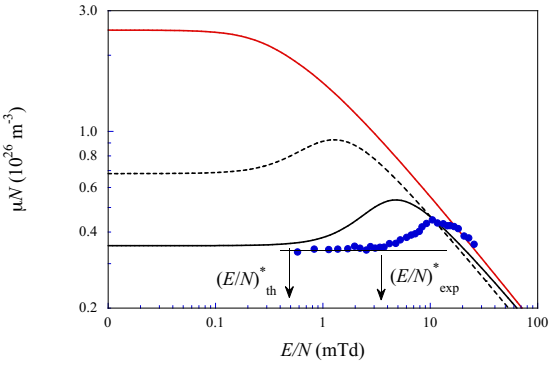

Fig. 6 Comparison of the prediction of the classical kinetic theory (red solid line) and of the heuristic model (black solid line) with the mobility data for $N = 9.48 \times 10^{26}\,\mathrm{m}^{-3}$ at $T = 4.2\,\mathrm{K}$.[18] The dashed line is the prediction of the heuristic model if only the infrared cut-off in the electron energy distribution function produced by the mobility edge is considered. The theroretically and experimentally determined threshold fields are indicated by arrows.

red solid line is the prediction of classical kinetic theory[30]. Its value at zero-field is roughly 10 times larger than the thermal value of the mobility. At high fields, however, when the electron energy is well above thermal, the experimental data and the teoretical prediction converge, as expected.

The heuristic model[34], on the contrary, dresses the classical kinetic formula with three multiple scattering effects: i) an infrared cut-off ε_c (known as *mobility edge energy*) in the electron energy distribution function due to quantum slef-interference of the electron wave packet leading to the so called *weak localization*[29,35,36]; ii) a density dependent shift of the electron ground state kinetic energy at the bottom of the conduction band in the gas that for helium is practically equal to $V_0(N)$[23,24,34]; and iii) an enhancement of the scattering cross sections via the static structure factor $S(k)$, in which k is the electron quantum wave number, that is due to correlations among atoms.[37] Explicit details of the heuristic model can be found in literature[31,34] and will not be repeated here.

The prediction of the (complete) heuristic model is shown as a black solid line in Fig. (6). At low field, the heuristic model almost agrees with the thermal mobility data. We remind that the experimental data in the figure are obtained for the lowest density, at which localized states still significantly contribute to the mobility, whereas the heuristic model is designed to describe the mobility of quasi-free electrons, only. Thus, we do not expect that the predicted μ_0 perfectly agrees with the experimental value as it occurs for higher T and/or lower N, as shown in literature.[34]

We note that increase of the measured mobility over its thermal value occurs at a much stronger field than that theoretically determined, $(E/N)^\star_{\mathrm{exp}} \gg (E/N)^\star_{\mathrm{th}}$. A great contribution to the mobility increase over its thermal values comes from the electric field induced shift of the electron energy distribution function. Whenever the field is so strong that the average electron energy gets larger than the mobility edge energy, a larger amount of quasi-free electron states contribute to the mobility. This is clearly shown by inspecting the dashed line in Fig. (6) that is computed if only the mobility edge cut-off out of the threee multiple scattering effects is considered. As the electric field gets so strong that the average electron energy becomes larger than the mobility edge energy, the Anderson localized electrons gets freed from the weak localizaton regime, and contribute to the increase of the mobiity.

If also the scattering cross section enhancement due to the two additional multiple scattering effects is taken into account (black solid line in the figure), it appears that electrons remain thermal at even stronger fields. However, even in this case, the threshold field value is weaker than experimentally observed. As the heuristic model describes only the quasi-free electron mobility, in order to explain why $(E/N)^\star_{\mathrm{exp}} \gg (E/N)^\star_{\mathrm{th}}$ we have to assume that in the presence of localized electrons states an even much greater average energy is required by electrons to escape self-trapping. The physical mechanisms to explain this fact are not completely clear. It might be that an increase of the average energy reduces the average residence time of the electrons over a density fluctuation, or the electric field, though it is tiny at microscopic scale, might increase the energy of the electron in the bubble so that they could be released from the cavity and participate to the transport as quasi-free electrons.

In any case, it is interesting to note that onset of localization always occurs whenever the energy gained by electrons from the electric field over one mean free path $\propto (E/N\sigma)$ is a constant fraction of the electron thermal energy. As the electron-atom scattering cross section σ is practically independent of the electron energy[41], it turns out that reduced electric field is proportional to the energy gained by electrons from the field. The previous conclusion is drawn by inspecting Fig. (7), in which we plot the ratio of the threshold electric field to the temperature, $(E/N)^\star/T$, for the lowest density, for which μ starts increasing over its thermal value μ_0, i.e., the lowest density at which a non negligible fraction of localized states measurably affects the mobility.
We see that within the accuracy of the determination of the threshold field, $(E/N)^\star/T$ is actually constant over an extended temperature range. It thus appears that a mechanism for the detectability threshold of localized states is the competition between thermal energy and energy gained from the field.

3 The optimum fluctuation model

The experimental evidence produced in the previous section has to be rationalized by assuming some physical model that allows the computation of the energetic and thermodynamic properties of the self-trapped states in comparison with the properties of the quasi-free ones. We will adopt here for its simplicity the optimum fluctuation model[23,24,42], in which the electron is localized within a square well potential. The minimum of the excess free energy of the localized state with respect to the quasi-free one is sought as a function of several parameters in order to find the most probable one. Clearly, it is a crude model, because, for instance, it neglects the possibility that there is a full distribution of bubble radii. In any way, in spite of its simplicity, it allows to grasp the essential

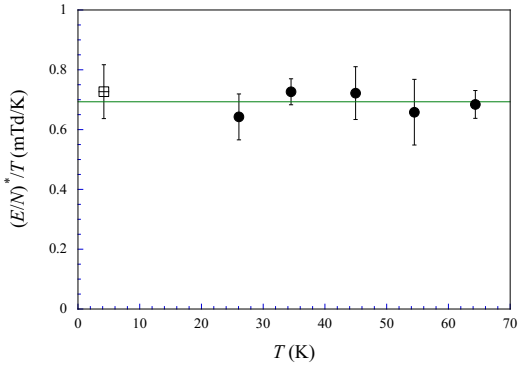

Fig. 7 Temperature dependence of the ratio of the energy gained by the electrons from the field over a mean free path $\propto (E/N)^\star$ to their thermal energy for the lowest density at which μ increases over its thermal value μ_0. Crossed square: [18]. Closed circles: [21,34,39].

physical features of the problem at hand and to make computations whose results can be directly compared to the experimental outcome. In the present section we will describe in detail this optimum flutuation model and present the computational results we obtained.

3.1 Quantum dynamics of localized electrons in helium gas

The first step to compute the excess free energy of the trapped state with respect to the quasi-free ones is to know the energy levels of electrons outside and inside the bubble.

Thermal, quasi-free electrons in helium gas at temperature T are endowed with the usual average kinetic energy $(3/2)k_BT$, in which k_B is the Boltzmann constant. However, as a consequence of multiple scattering effects, the electron kinetic energy is shifted by a density-dependent quantity $V_0(N)$ that represents the minimum energy at the bottom of the conduction band in the gas and the energy barrier for electron injection into the gas. Actually, V_0 should include the potential energy contribution due to the polarization interaction [23] but this contribution in helium can be neglected owing to its small polarizability.

V_0 can be computed within the Wigner-Seitz (WS) model by assuming that the electron quantum wave function $\psi(r)$ is (on average) locally invariant for translations of amplitude $2R_{WS}$, in which $R_{WS}(N) = (3/4\pi N)^{1/3}$ is the diameter of the WS sphere associated with each atom. Only s-wave states are sought because of the low temperatures of the experiments. The local translational invariance of $\psi(r)$ is enforced by requiring that $\psi(r)$ is anti-symmetric at the border of two adjacent WS spheres, thereby leading to the eigenvalue equation [24]

$$\tan\left[k_0\left(R_{WS} - \tilde{a}\right)\right] = k_0 R_{WS} \tag{1}$$

Here, k_0 represents the ground state momentum of the electron. [43] $\tilde{a}$ is the electron-atom scattering length. $V_0(N)$ is then computed as

$$V_0(N) = \frac{\hbar^2 k_0^2}{2m} \tag{2}$$

in which $\hbar$ is the reduced Planck's constant and m is the electron mass. The measurements of V_0 in helium [44] are in excellent agreement with eqn (2). $V_0(N)$ is positive and increases monotonically and superlinearly with increasing N, as shown in Fig. (8)

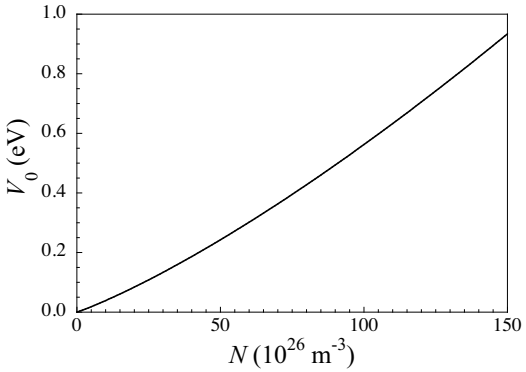

Fig. 8 V_0 as a function of N for helium from eqn 1 and eqn 2.

As the gas density and, hence, $V_0(N)$ fluctuate in space and time, electrons have lower energy in less-than-average density fluctuations. If the fluctuation is deep and broad enough, the residence time of the electron over the fluctuation can be quite long.

The dynamics of electron localization is still not undisputably clear yet, although it is accepted that it occurs on a timescale of a few ps. [45–47] There are suggestions that an electron makes a fast vertical transition to a virtual or resonant state in the continuum when it crosses a fluctuation of lower density. [4] Subsequently, a slow adiabatic process occurs in which the electron exerts a quantum pressure $\propto |\psi|^2$ on the fluctuation walls that pushes away the compliant gas atoms. This makes the fluctuation deeper and broader until an equilibrium configuration is reached, in which the electron is captured in the well giving origin to the self-localized state.

An alternative mechanism leading to the formation of self-localized states might be the Anderson-type localization due to strong disorder [48–51] that leads to an exponential decay of the electron wave function with distance. In this case these non-propagating states might be the precursors of electron bubbles (*incipient bubble*) because their residence time might be long enough to favor the broadening and stabilization of the fluctuation as a consequence of the medium compliance.

In any case, the stability of the localized state with respect to thermally activated fluctuations is determined by minimizing its Helmholtz free energy ΔA in excess of that of the quasi-free state. Thus, we will focus our attention only on the lowest, most probable state and neglect the possibility that excited states significantly contribute to the measured mobility.

Several approaches has been pursued to compute the excess free energy of localized states. Some of them are based on self-

consistent field approximation[43,52,53] or on density functional theory[54] and self-consistently provide also the well profile. Some others are simpler and assume a square profile for the well.[24,55] As we will show later, the precise details of the well profile are not very important as the wave function of the low-energy trapped electrons considerably spills over the bubble boundary into the gas for a quite long distance.

Thus, we adopt the optimum fluctuation model in which electrons are localized in spherically symmetric cavities of radius R with a square-well boundary. Note that, by minimizing ΔA we will find the most probable bubble radius but disregard the possible statistical distribution of radii of stable bubbles. The energy eigenvalue of the electron s-state in the cavity is obtained by solving the Schrődinger equation, provided that the potential energy of the electron in the cavity is known.

As there is no surface tension at the void-gas boundary in contrast with the liquid case, we assume that the cavity is not completely empty because some helium atoms, owing to their kinetic energy, can cross the boundary and can be accomodated in the cavity. As these atoms can dynamically interchange their position with atoms of the surrounding gas, we define an average filling fraction F as $F = N_i/N < 1$, in which N_i is the average gas density inside the bubble[6,21]. As a consequence, the ground state energy of the electron inside the bubble is reduced to

$$V_F(N) = V_0(N_i) = V_0(FN) < V_0(N) \tag{3}$$

Once in the cavity, electrons polarize the surrounding medium. By assuming the simplifying hypothesis that the electron resides in the exact center of the bubble, the polarization contribution to the electron energy, that turns out to be a function of density, filling fraction, and bubble radius, is given to first order by[6,24]

$$\mathscr{E}_P(N,R,F) = -\frac{1}{2}\frac{\alpha e^2}{4\pi\varepsilon_0 R}(1-F)N \tag{4}$$

In which $\alpha \approx 1.38 a_0^3$ is the atomic polarizability of helium, a_0 is the Bohr radius, and ε_0 is the vacuum permittivity. If the bubble were empty, i.e., $F = 0$, eqn (4) would yield the correct solvation energy of an ion immersed in a uniform medium of density N.[56]

By summing up eqn (3) and eqn (4) we obtain the potential energy of the electron in the bubble as

$$V_i(N,R,F) = V_F(N) + \mathscr{E}_P(N,R,F) \tag{5}$$

For the sake of completeness we have indicated the polarization contribution to the electron energy inside the bubble. However, owing to the small helium polarizability, this contribution is completely negligible, as it amounts, at most, to a few parts per thousand of $V_F(N)$ even for the smallest bubbles.

Only the lowest energy eigenvalue $\mathscr{E}_1$ of the s-state is required because of the low temperature of the experiments. If the s-wave wave function is written as $\psi(r) = u(r)/4\pi r$, $u(r)$ satisfies the following differential equations

$$\frac{\mathrm{d}^2}{\mathrm{d}r^2}u(r) = \begin{cases} -k_i^2 u(r) & \text{for } r < R \\ -k_o^2 u(r) & \text{for } r \geq R \end{cases} \tag{6}$$

with $k_i^2 = 2m[\mathscr{E}_1 - V_i(N,R,F)]/\hbar^2$ and $k_o^2 = 2m[V_0(N) - \mathscr{E}_1]/\hbar^2$.

The solutions for $u(r)$ are analytic

$$u(r) = \begin{cases} A\sin k_i r & \text{for } r < R \\ B\exp(-k_o r) & \text{for } r \geq R \end{cases} \tag{7}$$

where A and B are amplitude coefficients. By enforcing the continuity of the wavefunction and of its derivative at the bubble boundary $r = R$, we get the eigenvalue equation

$$\sqrt{H^2 - X^2}\tan X + X = 0 \tag{8}$$

in which $X = k_i R$ and $H^2 = (2m/\hbar^2)(V_0 - V_i)R^2$. A square well potential admits solutions only if its strength is $H \geq \pi/2$. Therefore, for any density and filling fraction there is a minimum bubble radius given by

$$R_0(N,F) = \left(\frac{\pi}{2}\right)\left[\frac{\hbar^2}{2m(V_0 - V_i)}\right]^{1/2}$$

For each value of N and F the energy eigenvalue is computed only for those bubbles whose radius exceeds R_0. If $X_1 \equiv X_1(N,R,F)$ is a solution of eqn (8), then the energy eigenvalue is given by

$$\mathscr{E}_1 \equiv \mathscr{E}_1(N,R,F) = \frac{\hbar^2}{2mR^2}X_1^2 \tag{9}$$

As a typical example of the solution of the Schrődinger equation for the electron in the cavity, we plot in Fig.(9) the normalized radial probability density $u^2(r)$ for an average density $N = 40 \times 10^{26}\,\mathrm{m}^{-3}$, filling fraction $F = 0.45$, and bubble radius $R = 27a_0$.

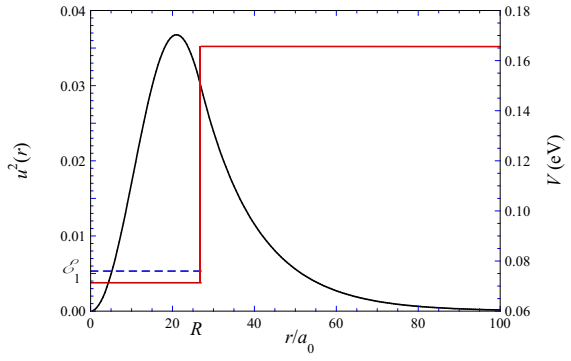

Fig. 9 Normalized probability density $u^2(r)$ (left scale) for an electron trapped in a bubble of radius $R = 27a_0$ for a gas density $N = 40 \times 10^{26}\,\mathrm{m}^{-3}$ and filling fraction $F = 0.45$. In red (right scale) the potential energy $V_i \approx 71\,\mathrm{meV}$ inside the bubble and $V_0 \approx 166\,\mathrm{meV}$ outside the bubble. The dashed line is the energy eigenvalue $\mathscr{E}_1 \approx 76\,\mathrm{meV}$.

As anticipated, the electron wave function spills over the boundary for a long distance, thereby making its details, either with a rounded or squared profile, largely irrelevant.

3.2 Thermodynamics of localized electrons

The isothermal volume work spent against the gas pressure to expand the bubble to its final size is

$$W = \frac{4\pi}{3} P(T,N) R^3 \left[1 - F - \frac{FN}{P(T,N)} \int_{FN}^{N} \frac{P(T,n)}{n^2} \, \mathrm{d}n \right] \qquad (10)$$

Here, $P(T,N)$ is the pressure given by the equation of state of helium gas[57].

Now, the excess free energy of the localized state with respect to the extended one is given by

$$\Delta A \equiv \Delta A(T,N,R,F) = \mathscr{E}_1 + W - (V_0 - V_i) \qquad (11)$$

and turns out to be a function of temperature, density, filling fraction, and bubble radius. To be rigorous, one should also add the surface energy contribution due the presence of the boundary by using the parachor equation to give an estimate of it.[58] However, it value is so small in any conditions that can be safely neglected.

Actually, ΔA should be averaged over all atomic configurations leading to self-localized states. This is evidently non viable and we use the optimum fluctuation approach[52] that yields the most probable state by minimizing the excess free energy with respect to bubble radius and filling fraction for each T and N.

As soon as a ΔA minimum appears, electron bubbles are mechanically stable, but only if this minimum becomes negative with $|\Delta A| > k_B T$ they are also stable against thermal fluctuations.

The optimum ratio of the trapped states fraction n_b to quasi-free fraction n_f is then obtained from the minimum excess free energy as

$$\frac{n_b}{n_f} = \exp(-\Delta A / k_B T) \qquad \text{with } n_f + n_b = 1 \qquad (12)$$

According to Young[22], the observed mobility μ is an average over the mobilities of the two most probable states. If μ_f and μ_b are the mobilities of the quasi-free and trapped electrons, respectively, and if $\mu_f \gg \mu_b$ as experimentally verified, μ is then given by

$$\mu = n_f \mu_f + n_b \mu_b \simeq \frac{1}{1 + \exp(-\Delta A / k_B T)} \mu_f \qquad (13)$$

3.3 Computational results

In order to get the most probable configuration, the excess free energy must be minimized with respect to both radius and filling fraction for each density at constant temperature.

For any given temperature T, the excess free energy is a monotonically increasing function of the bubble radius R below a minimum density whatever value the filling factor F may take on. As an example we plot in Fig. (10) the ratio of the excess free energy of the localized electron to the thermal energy $\Delta A(T,N,F,R)/k_B T$ at $T = 4.2\,\mathrm{K}$ for densities $N = 8$, 10, 12, and 15 (in units of $10^{26}\,\mathrm{m}^{-3}$) in a completely empty ($F = 0$) bubble. In this case the potential well is the deepest for a given bubble radius and leads to the most strongly bound electron state. The $N = 8$ and $N = 10$ curves, for instance do monotonically grow with increasing R. It happens because, for small enough N, the energy gain $V_i(N) - V_0(N)$ is not large enough to compensate for the isothermal work W. However, starting with the curve for $N = 12$ a minimum appears whose depth increases with increasing N. Only for N higher than a minimum density the excess free energy show a minimum for a given bubble radius whose location and strength depend on F and N. At first, the value of the ΔA minimum is positive but, by increasing N, it decreases, eventually becoming more and more negative. We note that this behavior is common to all values of filling fraction F at all temperatures. However, we want to stress the fact that this behavior does not rule out the presence of electron bubbles also at lower densities.

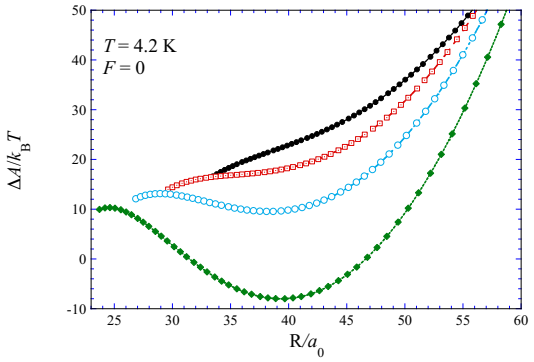

Fig. 10 Ratio of the localized state excess free energy to thermal energy $\Delta A/k_B T$ as a function of the bubble radius in units of Bohr radius R/a_0 for an empty bubble ($F = 0$) at $T = 4.2\,\mathrm{K}$. The average gas density is (from top) $N = 8$, 10, 12, and 15 in units of $10^{26}\,\mathrm{m}^{-3}$. The lines are only a guide to the eye.

The first step of the double optimizaton procedure is to minimize ΔA for any given T and N with respect to the bubble radius R with the filling fraction F as a parameter. As an example, we show in Fig. (11) the results obtained for $T = 10\,\mathrm{K}$ and $N = 34 \times 10^{26}\,\mathrm{m}^{-3}$ for several values of the filling fraction F. Similar results are obtained at all temperatures and densities.

We note that the empty bubble, defined by $F = 0$, is not necessarily endowed with the lowest value of the excess free energy. Actually, a partially empty bubble does show a smaller energy $V_i - V_0$ than an empty one that is compensated by a much smaller isothermal work required by its expansion. These two mechanisms are in competition and leads to the most negative excess free energy value occurring for a nonvanishing F value.

We first look for numerically minimizing $\Delta A(T,N,R,F)$ with respect to R, thereby yielding the coordinate of the minimum as $R_m(T,N,F)$ and the minimum of the excess free energy $\Delta A_m(T,N,R_m,F)/k_B T$. A typical example of the results is shown in Fig. (12).

It is interesting to examine the behavior of $\Delta A_m/k_B T$ as a function of F for several values of N at constant T as, for example, shown in Fig. (13) for $T = 50\,\mathrm{K}$. For lower densities, the minimum excess free energy is a monotonically decreasing function of the filling fraction F and does not show any, even positive, minimum. This dependence of $\Delta A_m/k_B T$ on F is a sign that the incipient

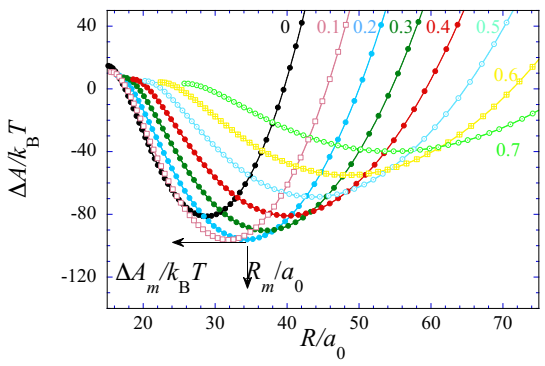

Fig. 11 Excess free energy in units of $k_B T$ computed as a function of the bubble radius for $N = 34 \times 10^{26}\,\mathrm{m}^3$ and $T = 10\,\mathrm{K}$. The curves are tagged with the value of the F parameter. $\Delta A_m/k_B T$ is the minimum excess free energy value for a given F and occurs at the optimum bubble radius R_m/a_0. The lines are only a guide for the eyes.

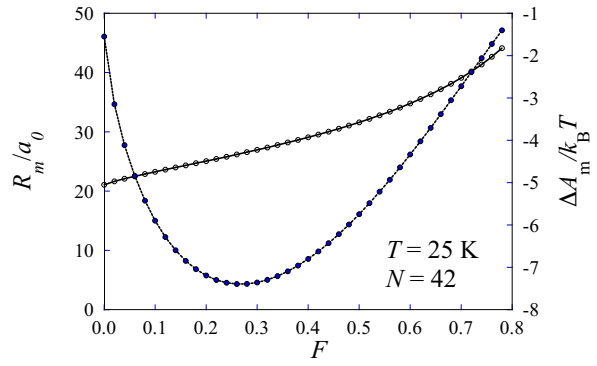

Fig. 12 Optimum bubble radius R_m in units of a_0 (open circles, left scale) and the exceess free energy value at R_m (closed symbols, right scale) as a function of F for $N = 42 \times 10^{26}\,\mathrm{m}^{-3}$ and $T = 25\,\mathrm{K}$. The solid lines are only a guide to the eye.

bubble is not stable. More and more atoms fill the cavity until it disappears. Only when N is increased a minimum of $\Delta A_m/k_B T$ appears at finite F. At first this minimum is positive showing that the bubble is mechanically stable but not stable against thermal fluctuations. Only for even higher N the minimum goes negative

The search for the minima corresponding to stable bubble states is the goal of the next minimization step when we look for the density dependence (at constant T) of the excess free energy minimum $\Delta A_m/k_B T$. By a fortunate chance, the dependence of $\Delta A_m/k_B T(T,N,R_m,F)$ on $R_m(T,N,F)$ is extremely well described by the analytical formula of the Morse-like potential[59]

$$\frac{\Delta A_m}{k_B T} = \frac{\Delta A_B}{k_B T} + b\left[1 - \mathrm{e}^{-(R_m - R_B)/\sigma}\right]^2 \qquad (14)$$

where b and σ are non relevant fitting parameters, whereas

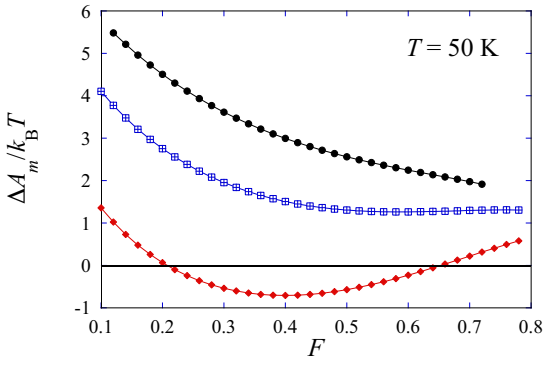

Fig. 13 Minimum excess free energy $\Delta A_m/k_B T$ as a function of F for $N = 41, 46$, and 52 (from top, in units of $10^{26}\,\mathrm{m}^{-3}$) for $T = 50\,\mathrm{K}$. The lines are only a guide to the eye.

$R_B = R_B(T,N)$ corresponds to the optimum bubble radius and $\Delta A_B/k_B T(T,N)$ is the most negative excess free energy value.

An example of this is shown in Fig. (14) for $T = 60\,\mathrm{K}$ and $N = 77, 78, 79$, and 80 in units of $10^{26}\,\mathrm{m}^{-3}$. Once more, similar results are obtained at all temperatures.

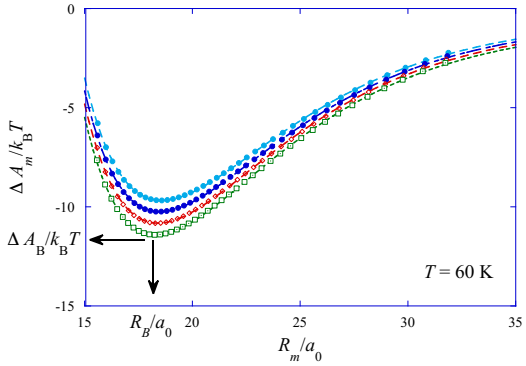

Fig. 14 Excess free energy $\Delta A_m/k_B T$ minimized with respect to both R and F as a function R_m for $T = 60\,\mathrm{K}$ for $N = 77, 78, 79$ and 80 in units of $10^{26}\,\mathrm{m}^{-3}$ (from top). Symbols: numerically computed values. Dashed lines: fit to eqn (14). The optimum values of radius and excess free energy obtained by the double minimization procedure are labeled R_B/a_0 and $\Delta A_B/k_B T$, respectively.

Some interesting features of the electron bubbles can now be deduced once the deepest values of the excess free energy have been computed. First of all, we plot the optimum radius R_B/a_0 as a function of the density for some temperatures in Fig. (15). At any temperature, R_B/a_0 decreases with increasing N, almost saturating at a constant value at high N. In particular, for $T \approx 5.2\,\mathrm{K}$, the limiting value is $R_B/a_0 \approx 39$ in reasonable agreement with the value $R_B/a_0 \approx 44$ obtained by a density functional approach for vapor at coexistence close to the critical temperature.[54]

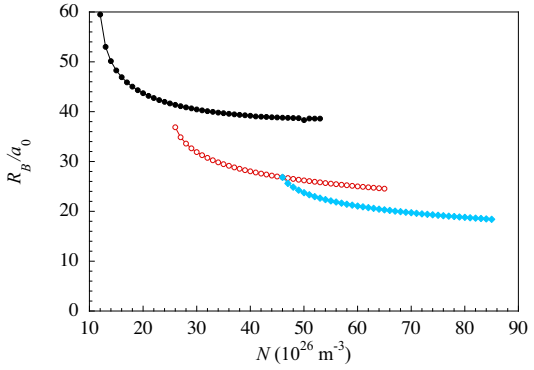

Fig. 15 Optimum bubble radius R_B/a_0 as a function of the density N for $T = 5.2, 18,$ and 50 K (from top). The lines are only a guide for the eye.

There is a simple rationalization for the behavior of R_B as a function of both and N and T. At constant T, R_B decreases with increasing N in order reduce the contribution of the mechanical work to the excess free energy. Similarly, as the pressure increases rapidly with T for a given N, R_B must be smaller at higher temperatures. Moreover, the R_B/a_0 curves progressively shift to higher density values as the temperature is increased just because of the corresponding shift of the localization onset.

Similar conclusions can be drawn by inspecting the density behavior of the optimum filling fraction F corresponding to deepest excess free energy minimum $\Delta A_B/k_\mathrm{B}T$ for some temperatures, shown in Fig. (16) Also in this case the optimal F curves shift to

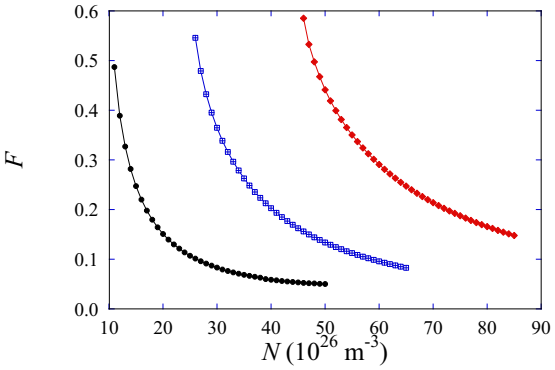

Fig. 16 The density dependence of the optimum filling fraction F corresponding to the deepest excess free energy minimum $\Delta A_B/k_\mathrm{B}T$ for $T = 4.2, 18,$ and 50 K (from left). The lines are only a guide for the eye.

higher N with increasing T for the same reason. At constant T, F monotonically decreases with increasing N. With increasing N the bubbles gradually become emptier as a result of the competition between the energy gain $V_i(N) - V_0(N)$ and the energy loss due to W. Moreover, F tends to saturate at large N to a non vanishing value of the order $2\% < F < 4.5\%$. This apparently means that the bubbles never become completely empty because of the absence of surface tension and of the nonvanishing kinetic energy of helium atoms.

Finally, we show the behavior of $\Delta A_B/k_\mathrm{B}T$ as a function of N for several temperatures in Fig. (17). We first note that, at constant

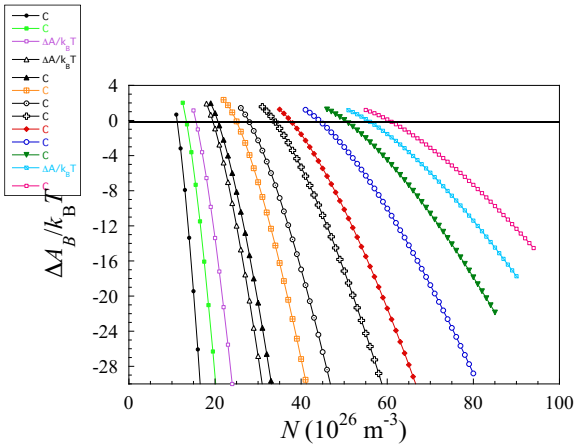

Fig. 17 Density dependence of the optimal excess free energy $\Delta A_\mathrm{B}/k_\mathrm{B}T$ for several temperatures $T\,(\mathrm{K}) = 4.2, 5.5, 7, 10, 11, 15, 18, 25, 30, 40, 50, 60,$ and 70 (from left). The solutions of $\Delta A_\mathrm{B}/k_\mathrm{B}T = 0$ give the locus of points where the localized- and quasi-free states are equiprobable. The solid lines are only guide for the eye.

T, the optimum excess free energy $\Delta A_\mathrm{B}/k_\mathrm{B}T$ rapidly decreases with increasing N. As a consequence, according to eqn (12), the fraction of localized states rapidly increases with increasing N.

When $\Delta A_\mathrm{B}/k_\mathrm{B}T = 0$, the two different states are equiprobable, i.e., they are present in the same amount. By inspecting Fig. (17), we note that the constant zero line intersects the excess free energy curves at increasingly larger densities as the temperature increases. The temperature dependent densities of the intersections represent the locus of points where the two states are equiprobable. It is also possible in a similar way to look for the temperature dependent densities corresponding to a given amount of localized states. By so doing, it is possible to determine a temperature dependent threshold density for the appearance of localized state in nonnegligible proportion. The curves shown in Fig. (3) have computed by inverting eqn 12 with $\Delta A = \Delta A_B$ for a required n_b/n_f ratio.

Figure (17) demonstrates that electron bubbles may form and be stable not only at low temperature but also at much higher temperatures provided that the density is large enough. We have limited the computation to $T = 80$ K because it is temperature closest to the highest one, at which the simultaneous presence of quasi-free- and localized states could still be observed[20,21,26,39].

For the sake of completeness, we additionally plot in Fig. (18) as a function of T the values of the filling fraction N_{50} and bubble radius R_{50} corresponding to the situation in which both states are equiprobable. We note that the optimal fillling fraction for the equiprobability condition is rather independent of T, whereas the corresponding bubble radius is a rapidly decreasing function of T

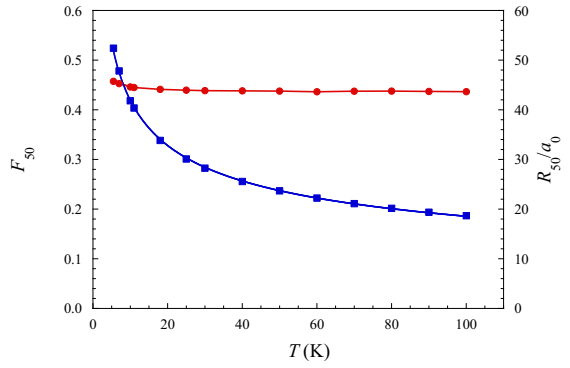

Fig. 18 Temperature dependence of the filling fraction F_{50} (red points, left scale) and bubble radius R_{50}/a_0 (blue squares, right scale) corresponding to the condition of equiprobability of quasi-free- and self-trapped states. The red line is a guide for the eye. The blue line is a $T^{-2/5}$ law.

with an approximate analytical form $T^{-2/5}$. This is a consequence of the fact that a smaller radius is required to keep relatively small the isothermal work to expand the bubble owing to the increase of P with increasing T for a given N.

Consistent with the previous observations is the average number n_d of atoms displaced from the interior of the bubble in conditions of equiprobability $n_d = (4\pi/3)R_{50}^3 N_{50}\,(1-F_{50}) \propto T^{-1/2}$, shown in Fig. (19), that rapidly decreases with increasing temperature.

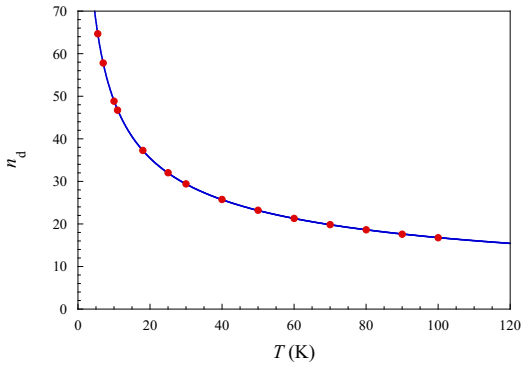

Fig. 19 Temperature dependence of the number of atoms displaced from the bubble interior in the condition of equiprobability. The solid line is a curve $\approx T^{-1/2}$

4 Conclusions

Thanks to the formulation of a very accurate prediction for the mobiity of quasi-free electrons in dense noble gases, we have reanalyzed literature data on electron mobility in dense helium gas with the goal to answer a long debated question whether electron self-trapping in bubbles occurs only at low temperature and above a given density threshold or whether some electrons are prone to self-localize as soon as they are injected into gaseous helium.

In our opinion, the answer is twofold. On one hand, from an experimentalist point of view we can only argue about a density threshold for the detectability of slow electrons localized in cavities. In this context we can claim that electron bubbles can be detected only if their concentration is such that the measured mobility drops below the theoretical prediction for quasi-free states well beyond the experimental accuracy. This arguments leads to the affirmative answer that localized states can be detected only above a temperature dependent, threshold density that can be deduced from the experimental data. A further conclusion from the experimental data is that the presence of electron bubbles is not limited to low temperatures but can be observed also at higher temperatures. The numerical results obtained by adopting the optimum fluctuation model (with the simplistic assumption that the bubbles have a square-well profile) confirm this point of view.

On the other hand, our computations (as well as those of other researchers[54] show that for every density there exists a minimum bubble radius that allows the (potential) formation of localized states. Moreover, we can claim that electron bubbles may always be created but that, in some thermodynamic conditions, their fraction is so tiny to be completely negligible. In this latter sense, we can speak of a threshold density for bubble formation.

However, some questions still remain unsolved. In particular, we might discuss about the nature of states with energy below the mobility edge energy. Are they localized in the Anderson sense? Can be they considered as precursors of incipient bubbles? We believe that more accurate and refined measurements in the density region where the electric field dependence of the mobility changes its behavior should help shedding light on these topics.

Author Contributions

All authors equally contributed.

Conflicts of interest

There are no conflicts to declare.

Acknowledgements

One of the authors (A.F.B.) acknowledges useful discussions with late Prof. M. Santini.

Notes and references

1 A. F. Borghesani, *Ions and Electrons in Liquid Helium*, Oxford University Press, Oxford, 2007, vol. 137.

2 J. L. Levine and T. M. Sanders, *Phys. Rev.*, 1967, **154**, 138–149.

3 L. Bruschi, G. Mazzi and M. Santini, *Phys. Rev. Lett.*, 1972, **28**, 1504–1506.

4 Y. Sakai, W. F. Schmidt and A. Khrapak, *Chem. Phys.*, 1992, **164**, 139–152.

5 A. F. Borghesani, L. Bruschi, M. Santini and G. Torzo, *Phys. Rev. A*, 1988, **37**, 4828–4835.

6 A. F. Borghesani and M. Santini, *Phys. Rev. A*, 1990, **42**, 7377–7388.

7 P. Krebs and U. Lang, *J. Phys. Chem.*, 1996, **100**, 10482–10489.
8 P. Krebs, V. Giraud and M. Wantschik, *Phys. Rev. Lett.*, 1980, **44**, 211–213.
9 P. Krebs and M. Heintze, *J. Chem. Phys.*, 1982, **76**, 5484–5492.
10 T. Wada and G. R. Freeman, *J. Chem. Phys.*, 1980, **72**, 6726–6730.
11 G. Grimm and G. Rayfield, *Phys. Lett. A*, 1975, **54**, 473–475.
12 Y. Sakai, H. Böttcher and W. Schmidt, *J. Electrostatics*, 1982, **12**, 89–96.
13 A. A. Levchenko and L. P. Mezhov-Deglin, *J. Low Temp. Phys.*, 1992, **89**, 457—463.
14 V. Giraud and P. Krebs, *Chem. Phys. Lett.*, 1982, **86**, 85–90.
15 T. Ichikawa and H. Yoshida, *J. Chem. Phys.*, 1981, **75**, 5432—5437.
16 C. C. Grimes and G. Adams, *Phys. Rev. B*, 1990, **41**, 6366–6371.
17 C. C. Grimes and G. Adams, *Phys. Rev. B*, 1992, **45**, 2305–10.
18 K. W. Schwarz, *Phys. Rev. B*, 1980, **21**, 5125–5136.
19 H. R. Harrison, L. M. Sander and B. E. Springett, *J. Phys. B: Atom. Molec. Phys.*, 1973, **6**, 908–917.
20 J. A. Jahnke, M. Silver and J. P. Hernandez, *Phys. Rev. B*, 1975, **12**, 3420–3427.
21 A. F. Borghesani and M. Santini, *Phys. Rev. E*, 2002, **65**, 056403.
22 R. A. Young, *Phys. Rev. A*, 1970, **2**, 1983–1986.
23 B. E. Springett, J. Jortner and M. H. Cohen, *J. Chem. Phys.*, 1968, **48**, 2720–2731.
24 T. Miyakawa and D. L. Dexter, *Phys. Rev.*, 1969, **184**, 166–172.
25 R. Grűnberg, *Z. Naturforsch. A*, 1969, **24**, 1838–1839.
26 A. Bartels, *Appl. Phys.*, 1975, **8**, 59–64.
27 T. F. O'Malley, *J. Phys. B: Atom. Molec. Phys.*, 1980, **13**, 1491–1504.
28 G. L. Braglia and V. Dallacasa, *Phys. Rev. A*, 1982, **26**, 902–914.
29 I. T. Iakubov and A. Y. Polischuk, *J. Phys. B: Atom. Molec. Phys.*, 1982, **15**, 4029–4041.
30 L. G. Huxley and R. W. Crompton, *The Diffusion and Drift of Electrons in Gases*, Wiley, New York, 1974.
31 A. F. Borghesani, M. Santini and P. Lamp, *Phys. Rev. A*, 1992, **46**, 7902–7909.
32 A. F. Borghesani and M. Santini, *Phys. Rev. A*, 1992, **45**, 8803–8810.
33 A. Borghesani, *J. Electrostatics*, 2001, **53**, 89–106.
34 A. F. Borghesani, *Atoms*, 2021, **9**, 52.
35 A. Y. Polischuk, *Physica B+C*, 1984, **124**, 91–95.
36 G. Ascarelli, *Condens. Matter*, 1992, **4**, 60554072.
37 J. Lekner, *Phil. Mag.*, 1968, **18**, 1281–1286.
38 F. Aitken, Z.-L. Li, N. Bonifaci, A. Denat and K. von Haeften, *Phys. Chem. Chem. Phys.*, 2011, **13**, 719–724.
39 A. M. De Riva, *MSc thesis*, University of Padua, Padua, Italy, 1994.
40 V. M. Atrazhev and I. T. Iakubov, *J. Phys. D: Appl. Phys.*, 1977, **10**, 2155–2163.
41 T. F. O'Malley, *Physical Review*, 1963, **130**, 1020–1029.
42 A. G. Khrapak, Y. Sakai, E. H. Böttcher and W. F. Schmidt, *IEEE Transactions on Electrical Insulation*, 1991, **26**, 582–585.
43 J. P. Hernandez and L. W. Martin, *Phys. Rev. A*, 1991, **43**, 4568–4571.
44 J. R. Broomall, W. D. Johnson and D. G. Onn, *Phys. Rev. B*, 1976, **14**, 2819–2825.
45 J. P. Hernandez and M. Silver, *Phys. Rev. A*, 1970, **2**, 1949–1954.
46 M. Rosenblit, *Phys. Rev. Lett.*, 1995, **75**, 4079–4082.
47 M. Rosenblit and J. Jortner, *J. Phys. Chem. A*, 1997, **101**, 751–757.
48 P. W. Anderson, *Phys. Rev.*, 1958, **109**, 1492–1505.
49 M. Cutler and N. F. Mott, *Phys. Rev.*, 1969, **181**, 1336–1340.
50 T. P. Eggarter and M. H. Cohen, *Phys. Rev. Lett.*, 1970, **25**, 807–810.
51 J. P. Hernandez, *Phys. Rev. A*, 1973, **7**, 1755–1765.
52 A. G. Khrapak and I. T. Yakubov, *Sov. Phys. Usp.*, 1979, **22**, 703–726.
53 K. F. Volykhin, A. G. Khrapak and W. F. Schmidt, *JETP*, 1995, **81**, 901–908.
54 D. Jin and W. Guo, *J. Chem. Phys.*, 2012, **136**, 244510.
55 A. L. Fetter, *The Physics of Liquid and Solid Helium*, Wiley, New York, 1975.
56 M. Born, *Z. Phys.*, 1920, **1**, 45–48.
57 R. D. McCarty and V. D. Arp, in *A New Wide Range Equation of State for Helium*, ed. R. W. Fast, Springer US, Boston, MA, 1990, pp. 1465–1475.
58 J. O. Hirschfelder, C. Curtiss and R. Bird, *Molecular Theory of Gases and Liquids*, Wiley, New York, 1964.
59 P. M. Morse, *Phys. Rev.*, 1929, **34**, 57–64.